STABILITY ANALYSIS OF DOW S110(21<S

RUTH DGANI, DAVE VAN BUREN & ALBERTO NORIEGA-CRESPO

INFRARED PROCESSING AND ANALYSIS CENTER, JET PROPULSION LABORATORY

CALIFORNIA INSTITUTE OF TECHNOLOGY

POSTAL ADDRESS: IPAC, CALTECH 1.00-22, PASADENA, CA 91125

INTERNET: KNILL, DAVE, ALBERTO@IPAC.CALTECH.EDU

ABSTRACT

We present a linear stability analysis of bow shocks created by the interaction of a spherical wind moving with respect to its surrounding medium. The bounding shocks are assumed isothermal and with Mach number $M = \infty$. Following Soker (1990) we study the evolution of short wavelength perturbations. We find that the motion is unstable in this limit. Moreover, the ratio of the wind velocity v_w to the star velocity v_* characterizes the stability properties. Dow shocks with fast winds for which $v_*/v_w << 1$ are more stable than bow shocks with slow winds i.e. $v_*/v_w \gg 1$.

1. INTRODUCTION

Bow shocks appear in a variety of astrophysical situations, but perhaps some of the most spectacular are those associated with "runaway" stars (Van Buren 1993). In these systems, bow shocks develop as OB stars move supersonically through their ambient media when their stellar winds are confined by ram pressure (Van Buren et al. 1990). The interaction region between the wind and the circumstellar shocked gases is bounded by two shocks in which the flows slow down from supersonic to subsonic velocities. The width of the interaction region depends on the efficiency of the cooling processes as well as on the Mach numbers of the interacting flows. For efficient cooling the interaction zone narrows with increasing Mach number, becoming in the limit infinitesimally thin. The wind velocities of OB stars are $\sim$ 1000--3000 km s^{-1}, which lead to very high post-shock temperatures at the wind shock. A variety of cooling mechanisms are likely to operate, among them turbulent mixing via Kelvin-Helmholz instabilities, thermal conduction and radiation 1o sscs, resulting in a narrow interaction region. Studies of the closely related stellar wind bubbles indicate that strong losses can indeed occur (Vail Buren 1 986).

In this paper we perform a linear stability analysis of a bow shock created by a spherical wind interacting with a uniformly flowing interstellar medium. We assume both flows are isothermal with high Mach number, a situation likely to be relevant for bow shocks around runaway stars. Similar flow conditions occur in colliding winds in relatively close binary systems (Stevens, Blondin & Pollock 1992; Bainanov, Pilyugin & Usov 1990).

There is a whole class of astrophysical gas dynamic problems in which a stellar wind or a supernova explosion results in the formation of a high density zone. If this zone is thin relative to its radius, and if it is bounded by sharp boundaries, the problem of its evolution can be solved by treating the zone as a surface of zero thickness. The zero thickness shell approximation was used to study the evolution of various flows both spherically symmetric

and axisymmetric (see Giuliani 1982 for references on the various application of the zero thickness model). Soker (1990) used the zero thickness shell approximation to investigate the stability properties of the accretion line found in the wake of a gravitating object embedded in a uniform flow. Dgani, Walder & Nussbaumer (1 993) and Dgani (1993), follow Soker (1 990) and usc the same approximation to perform a linear stability analysis of the collision front between two identical winds in a double star system. The collision front is unstable in this limit. Dgani & Soker (1994) follow the same instability to the nonlinear regime using numerical simulations. They also compare the accretion line case, investigated numerically by Soker (1991) to the colliding wind binary case, and find that tile accretion line shows much stronger instability. The large growth rates of disturbances in the accretion process are due to the presence of the gravitating object. Vishniac (1994) finds a different kind of instability occurring in thin shells bounded by two shocks that is both nonlinear and local (the nonlinear thin shell inst ability , hereafter NTSI). Vishniac's imitability is related to the shear inside the thin shell layer and and has highest growth rates for modes with wavelength of the order of the thickness of the shell.

In this paper we perform the linear stability analysis of bow shocks in the zero thickness shell limit. We find indeed that bow shocks are unstable in this limit. In §2 we usc Giuliani's formulation (Giuliani 1982) of the thin shell model to derive the hydrodynamical equations. In §3 we perform the stability analysis, obtain the dispersion relation for short wavelength disturbances and explain the physical nature of the instability we find. In §4 we consider astrophysical systems where this instability may be present. We find that the stability properties of stellar wind bow shocks depend 011 a single parameter, the ratio of the wind velocity, v_w, to the stellar (or moving medium) velocity, v_*. Bow shocks with $v_*/v_w << 1$ are more stable than those with $v_*/v_w >> 1$.

2. THE HYDRODYNAMICAL EQUATIONS

We treat the case of a zero thickness collision front in the coordinate system (r, θ, ϕ) of Baranov, Krasnobaev & Kulikovskii (1971). The wind source is placed at the origin, r is the distance from the origin, 19 is the angle measured from the positive xy-plane, and ϕ is the azimuthal angle around the z-axis (see Fig. 1). For simplicity we assume that the flow is independent of ϕ, in other words, we consider a collision surface S of the form

$$\mathsf{S} = S(r(\theta,t),\theta,\phi). \tag{2.1}$$

The undisturbed collision surface is

$$S_0 = S(r_0(\theta),\theta,\phi)\ , \tag{2.2}$$

where $r_0(\theta)$ is given as the numerical solution of a complicated ordinary differential equation in Baranov et al. (1971). The surface area of a surface element between θ and $\theta + \Delta\theta$ and ϕ and $\phi + \Delta\phi$ is

$$\Delta S = r \sin\theta \sqrt{r_\theta^2 + r^2}\, \Delta\theta \Delta\phi \tag{2.3}$$

where the subscript 6' denotes the derivative with respect to θ. The tangent to the line $r(\theta,t)$ in the zx plane is

$$\hat{l} = \frac{\hat{z}(r_\theta \cos\theta - r \sin\theta) + \hat{x}(r_\theta \sin\theta + r\cos\theta)}{\sqrt{r_\theta^2 + r^2}}\ , \tag{2.4}$$

The normal to the line $r(\theta,t)$ in the zx plane is

$$\hat{n} = \frac{\hat{z}(r_\theta \sin\theta + r\cos\theta) + \hat{x}(-r_\theta \cos 0 + r\sin\theta)}{\sqrt{r_\theta^2}} \quad \text{-i-1,2} \quad \text{-----} \quad \text{-----}\ . \tag{2.5}$$

For the undisturbed bow Shock

$$\hat{l}_0 \quad \frac{\hat{z}(r_0' \cos\theta - r_0 \sin\theta) + \hat{x}(r_0' \sin\theta \text{ -i } r_0 \cos\theta)}{\sqrt{r_0'^2 + r_0^2}} \tag{2.6}$$

and

$$\hat{n}_0 = \frac{\hat{z}(r_0' \sin\theta + r_0 \cos\theta) + \hat{x}(-r_0' \cos\theta + r_0 \sin\theta)}{\sqrt{r_0'^2 + r^2}} , \tag{2.7}$$

where the prime denotes the derivative with respect to θ.

Conservation of Mass

The change of mass in the surface element AS is a result of fluxes coming from the wind source and from the ambient medium, as well as from matter flowing along the surface into and out of the element.

The mass flux into AS from the source is

$$\dot{\sigma}_w \, \Delta S = \rho_w(r_0)(v_w \hat{r} - \vec{v}) \cdot \hat{n} \, \Delta S , \tag{2.8}$$

where $\vec{v}$ is the velocity of a material element on the surface. We designate the source quantities with subscript w.

The mass flux into AS from the ambient medium is

$$\dot{\sigma}_a \, \Delta S = \rho_a(v_* \hat{z} + \vec{v}) \cdot \hat{n} \, \Delta S \tag{2.9}$$

where ρ_a is the density of the ambient medium and v_* is the stellar velocity with respect to the ambient medium.

The mass flowing into AS by motion in the surface is

$$\partial_\theta \sigma \, (\vec{v} - \partial_t r \, \hat{r}) \cdot \hat{l} \, r \sin\theta \Delta\theta \Delta\phi , \tag{2.10}$$

where σ, $\vec{v}$ are the surface density and the velocity at the point r, θ, ϕ on the surface S. $\vec{v} - \partial_t r \, \hat{r}$ is the velocity of gas with respect to the control surface (Giuliani 1982).

The change of the mass in the surface element AS with time is

$$\partial_t(\sigma \Delta S) . \tag{2.11}$$

Calling $\dot{\sigma}$ the sum of the mass fluxes from the source and from the ambient medium divided by $\Delta\theta\Delta\phi$, we obtain the equation for conservation of mass:

$$\partial_t \left(\sigma r \sin\theta \sqrt{r_\theta^2 + r^2} \right) + \partial_\theta \left(\sigma \left(\vec{v} - \partial_t r \, \hat{r} \right) \cdot \hat{l} \, r \sin\theta \right) = \dot{\sigma} \tag{2.12}$$

Conservation of Momentum

The change of momentum in the surface element AS is a result of fluxes coming from the source and from the ambient medium, as well as from matter flowing along the surface into and out of the element.

The momentum flux into AS from the source is

$$\rho_w(r_0)(v_w \hat{r} - \vec{v}) \cdot \hat{n} \text{ AS } v_w \hat{r} \, . \tag{2.13}$$

The momentum flux into AS from the ambient medium is

$$\rho_a(v_* \hat{z} + \vec{v}) \cdot \hat{n} \text{ AS } v_* (-\hat{z}) \, . \tag{2.14}$$

The momentum flowing into AS by motion along the surface is

$$\partial_\theta (\sigma \left(\vec{v} - \partial_t r \, \hat{r} \right) \cdot \hat{l} \, r \sin\theta \, v) \Delta\theta\Delta\phi \, . \tag{2.15}$$

The change of the momentum in the surface element AS with time is

$$\partial_t (\sigma \Delta S \, \vec{v}) \, . \tag{2.16}$$

Calling $\dot{\vec{P}}$ the vector sum of the momentum fluxes from the source and from the ambient medium we obtain the equation of conservation of momentum:

$$\partial_t \left(\sigma \, r \sin\theta \sqrt{r_\theta^2 + r^2} \; \vec{v} \right) + \partial_\theta (\sigma \left(\vec{v} - \partial_t r \, \hat{r} \right) \cdot \hat{l} \, r \sin\theta \; \vec{v}) = \dot{\vec{P}} \tag{2.17}$$

Following Guiliani (1982), we write the Euler equation obtained by subtracting the mass conservation equation times $\vec{v}$ from the equation of conservation of momentum and dividing by $r \sin\theta\sqrt{r_\theta^2 + r^2}$:

$$\sigma\partial_t\vec{v} + \sigma(\vec{v} - \partial_t r\,\hat{r})\cdot\hat{l}\frac{1}{\sqrt{r^2 + r_\theta^2}}\partial_\theta\vec{v} = \vec{\pi} \tag{2,18}$$

where

$$\vec{\pi} = \frac{\dot{\vec{P}} - \dot{\sigma}\vec{v}}{r\sin\theta\sqrt{r_\theta^2 + r^2}} \tag{2.19}$$

is the force applied to the material in the surface element by f] uxcs from the wind source and the ambient medium, and

$$\frac{1}{\sqrt{r^2 + r_\theta^2}}\partial_\theta\vec{v} = \frac{1}{\sqrt{r^2 + r_\theta^2}}\left(\hat{n}\partial_\theta(\vec{v}\cdot\hat{n}) + \hat{l}\partial_\theta(\vec{v}\cdot\hat{l})\right) + \frac{1}{R_c}\left(\hat{l}(\vec{v}\cdot\hat{n}) - \hat{n}(\vec{v}\cdot\hat{l})\right) \tag{2.20}$$

In the last equation R_c is the radius of curvature of the bow shock

$$R_c = \frac{(r^2 + r_\theta^2)^{3/2}}{r^2 + 2r_\theta^2 - rr_{\theta\theta}} \tag{2.21}$$

With $\vec{v} = v_l\hat{l}_0 + v_n\hat{n}_0$ the evolution equations for v_l and v_n are obtained by multiplying equation 2.18 by $\hat{l}_0$ and $\hat{n}_0$ respectively.

The Kinematic Relation

The velocity of a material element on the bow s] ıock is the total time derivative of the coordinate of this element $r(\theta(t), t) = r_0(\theta(t)) + r_1(\theta(t), t)$. r_1 is the perturbation in r and is assumed to be much smaller than r_0.

$$\vec{v} = \left(r_l + \frac{d\theta}{dt}r_\theta\right)\hat{r} + r\frac{d\theta}{dt}\hat{\theta} \tag{2.22}$$

where $\frac{d\theta}{dt} = (\vec{v}\cdot\hat{\theta})/r$. With $\vec{v} = v_l\hat{l}_0 + v_n\hat{n}_0$ the last equation gives after a little algebra:

$$v_n = \frac{r_0}{\sqrt{r_0'^2 + r_0^2}}\left(\partial_t + \frac{v_{l0}}{\sqrt{r_0'^2 + r_0^2}}\partial_\theta\right)r_1 - \frac{v_{l0}r_0'\,r_1}{r_0'^2 + r_0^2} \tag{2.23}$$

Note that $\theta(t)$ is a function of time because we follow a particle (Lagrangian view).

3. THE STABILITY ANALYSIS

3.1 The Dispersion Relation

Following Soker (1990), we consider small perturbations to the steady state solution we designate by $r = r_0(\theta)$, $\sigma = \sigma_0(\theta)$, $v_l = \vec{v} \cdot \hat{l}_0 = v_{l0}$. Considering short wavelength disturbances, i.e. the wavelength of the disturbances is smaller than the other length scales in the problem $\sigma/\partial_l\sigma$ etc. we use the WKB approximation (Brillouin 1926, Wentzel 1926, Kramer 1926) and write the physical quantities in the form:

$$r(\theta,t) = r_0(\theta) + \Delta r(\theta) \exp\left[i\omega t + i\int k(l)dl\right]$$

$$\sigma(\theta,t) = \sigma_0(\theta) + \Delta\sigma(\theta) \exp\left[i\omega t + i\int k(l)dl\right]$$

$$v_l(\theta,t) = v_{l0}(\theta) + \Delta v_l(\theta) \exp\left[i\omega t + i\int k(l)dl\right] \qquad (3.1)$$

$l(\theta)$ is the length of the bow shock curve $r_0(\theta)$, $dl/d\theta = \sqrt{r_0'^2 + r_0^2}$. The amplitudes of the perturbations Δr, $\Delta\sigma$ and Δv_l and the wave number k are slowly varying functions of l on the scale length 11 of the steady state solution, while $kH >> 1$. Substituting the above relations in the hydrodynamical equations 2.12, 2.18 and 2.23 while keeping only the high order terms in k we obtain a relation between w and k

$$w + v_{l0}k = \sqrt{k}b \qquad (3.2)$$

where b is the solution to the algebraic equation:

$$\frac{\dot{\pi}_l}{\sigma_0}\frac{v_{l0}^2}{R_{c0}} + \left(b^2 + iv_{l0}\frac{dv_{l0}}{dl}\right)\left(b^2 - i\frac{\dot{\pi}_n}{\sigma_0}\right) = 0 \qquad (3.3)$$

and

$$\dot{\pi}_l = (\dot{\vec{\pi}}_1 \cdot \hat{l}_0)/\partial_l r_1$$

$$\dot{\pi}_n = (\dot{\vec{\pi}}_1 \cdot \hat{n}_0)/\partial_l r_1 \qquad (3.4)$$

$r_1 = r(\theta, t) - r_0(\theta)$ and $\vec{\pi}$ is given in equation (2.19). Keeping only terms of highest order in k,

$$\dot{\vec{\pi}}_1 = (\dot{\sigma_{w1}} v_w \hat{r} - \dot{\sigma_{a1}} v_* \hat{z}) \tag{3.5}$$

where

$$\dot{\sigma}_{w1} = \rho_w(r_0)(v_w \hat{r} - \text{u}) \text{“(h} - \hat{n}_0) , \tag{3.6}$$

$$\dot{\sigma}_{a1} = \rho_a(v_* \hat{z} + \vec{v}) . (\hat{n} - \hat{n}_0) , \tag{3.7}$$

and

$$\hat{n} - \hat{n}_0 = \hat{r} \cdot \hat{n}_0 \, \partial_l r_1 \, \hat{l}_0 \tag{3.8}$$

$\dot{\sigma_{w1}}$ and $\dot{\sigma_{a1}}$ are the disturbances in the mass flux from the ambient medium and the wind source respectively because of the tilt in the surface. From equations (3.4) to (3.8) we see that to highest order in k the change in the accretion of matter 1 because of the orientation the bow shock surface dominates the source terms $\dot{n}_l$ and $\dot{\pi}_n$ in equation (3.3).

There are 4 roots to this equation, 2 of them have negative imaginary part and result in exponential growth. Since the oscillation period is of order k^{-1} and is shorter than the growth time of the perturbation $\sim 1/k^2$ the instability described by the dispersion relation 3.2 is an overstability.

3.2 The Physical Nature of the Instability

in order to track the origin of the instability we first note that when the radius of curvature is large we reproduce the results obtained by Dgani et al (1993) for the case of two colliding winds. In this case the motion normal to the surface (transverse motion) is independent of the motion in the direction of the surface (longitudinal motion). The dispersion relation 3.2 gives two distinct, modes longitudinal and transversal. The evolution of the longitudinal modes is governed by the relation

$$\omega + v_{l0} k = \sqrt{- ikv_{l0} \frac{dv_{l0}}{dl}} , \tag{3.9}$$

which is similar to the dispersion relation for the radial modes in the planar shock (Dgani et al. 1993 equation 24). The evolution of the transverse modes is governed by the relation

$$\omega + v_{l0}k = \sqrt{ik\frac{\dot{\pi}_n}{\sigma_0}}\ , \tag{3.10}$$

which is similar to the dispersion relation for the transverse modes in the planar shock (Dgani et al. 1993 equation 31). The longitudinal modes do not depend on the sources and their instability results from the acceleration along the undisturbed surface (Soker 1990). The dispersion relation for the transverse modes contains the source term $\dot{\pi}_n$, i.e. the motion normal to the surface changes the fluxes of momentum from both sources and results in a net force on the element.

As equation **3,3** shows the decoupling of the eigen modes occurs when the first term on the RHS is zero. This term depends on the centrifugal acceleration. While in the planar case changes in the surface density created motion only in the surface itself, here the centrifugal force operates out of the surface and couples the motion in the surface to that normal to it.

The instability described here is of a very similar nature to the colliding wind binary instability described by Dgani et al. (1993). It arises from the fact that density fluctuations in the bow shock surface lead to fluctuations in the transverse acceleration. When the wind stream collides with the ambient medium stream, the shocked slab tends to oscillate away from the equilibrium position, accelerated outward by the oblique accretion of the streams. We therefore name it the transverse acceleration instability (q'Al).

3.3 Relation to other thin shell instabilities

Our analysis assumes that the thin shell is bounded by two shocks i.e. that the wind shock is also isothermal.

A set of overstabilities related to thin shells bounded on one side by a shock and

on the! other side by a hot high pressure gas have been investigated by Vishniac (1983), Ryu & Vishniac (1987), and Mac-Low & Norman (1993), These instabilities are driven by the inability of thermal pressure (which always acts normal to the surface) to balance the ram pressure (which is directed along the shell velocity vector). Ripples in the shell will chive motion within the shell and concentrate matter in "valleys" (see e.g. in Mac-Low and Norman 1993 Figure 1). T] ie ram pressure then decelerates the diluted peaks more rapidly reversing the direction of the flow causing valleys to turn into peaks. Vishniac (1983) showed that peaks and valleys grow in each cycle.

If the two bow shocks around runaway stars are really confined by two isothermal shocks, then the only other dynamical instability that is competing with the one described here. is the NTSI described by Vishniac (1994). The NTSI is related to shear motions in the thin shell invoked by rippling it. Its growth rates are highest for modes of wavelength of the order of the shell thickness and are at most only slightly higher than $c_s k$ where c_s is the sound speed in the shell.

Following Vishniac (1994), who compared the NTSI with the zero thickness colliding wind binaries instability (Dgani et al. 1993), we compare the growth rates of the NTSI with those of the TAI. The growth rate for the TAI can be approximated as $C(l)v_{l0}(k/l)^{1/2}$ (see below eqn. 4, 1), For $l \leq l_{s0}$ where $l_{s0} = r_0(\theta = 0)$ is the stand of]' distance, v_{l0} is a linear function of 1 and the growth rate can be written as $V(lk)'^{12}/l_{s0}$, where V is the minimum of v_* and v_w and l_{s0} is the stand off distance. The instability described here has larger rates for $\lambda > \delta l_{s0}/l$ where $\delta = l_{s_0}/(V/c_s)^2$ is the thickness of the shell. The last relation means that the c.loser to the nose of the bow shock we get the longer the wavelength has to be so that the TAI will grow faster than the NTSI. However, for 1 of the order of l_{s0} the TAI wins for wavelengths longer than the thickness of the shell. However, since the fluid moves from the front of the bow shock back, so that small wavelegth disturbances near the bow evolve into large wavelegth disturbances on the sides, it seems likely that the NTS1

playes an important role in providing initial conditions for the TA1.

4. DISCUSSION

The instability growth rate versus v_*/v_w relationship

The observed morphology along bow shock structures could be the result of the instability described here. In order to apply the above analysis to real systems we consider the approach by Dgani & Soker (1994), and follow a fluid element as it moves along the bow shock, The perturbation amplitude of a parcel of material flowing from l_1 to 1_2 along the bow shock is:

$$\log\left[\frac{A(l_2)}{A(l_1)}\right] = \int \frac{Re(i\omega)}{v_{l0}} dl \sim C(l_{ave})((l_2/\lambda)^{1/2} - (l_1/\lambda)^{1/2}) \qquad (4.1)$$

where $l_{ave} = (l_1 + l_2)/2$. In the last expression we assume $12\text{--}11 \leq r_0(\theta = 0)$. $C(l(\theta)) = 2Re(ib)\sqrt{2\pi l(\theta)}/v_{l0}$ is a slowly varying function of l, where! b is one of the 4 roots of equation (3.3) , for which $Re(ia)$ is the biggest. We substituted in the dispersion relation *(3.2)* $k = 2\pi/\lambda$, where λ is the wavelength.

$C(l)$ is an increasing function of $\alpha = v_*/v_w$. Bow shocks with a bigger ratio α have higher growth rates and are therefore less stable, In figure 2 we plot C as a function of $\log \alpha$ for the angle $\theta = 120°$. Using equation (4. 1) and Figure 2, the amplitude growth for a bow shock with $v_*/v_w = 0.01$ is $\exp(4.3 - 1.5) \sim 16$ times smaller than that of a bow shock with $v_*/v_w = 100$, and is ~ 3 times smaller than that of a bow shock with $v_*/v_w = 1$ at $\theta = 120$.

Comparison with Bow Shocks

Bow shocks in astronomy are ubiquitous (Van Buren 1993), and since the ratio of velocities α is in principle an easily measured quantity, it is interesting to consider some astrophysical phenomena where the above process may be occurring and study their behavior according to their different α ratio.

Ram pressure balance between the stellar winds of runaway OB stars and the surrounding gas leads to the formation of bow shocks (Van Buren & McCray 1988). Nearly one third of the runaway stars seem to be surrounded by bow shocks due to this process (Van Buren, Noriega-Crespo & Dgani 1995). At optical wavelengths these bow shocks are difficult to detect, due to their small column densities; however the dust trapped in the bow shock shell re-radiates efficiently about 1% of the star's bolometric luminosity at far infrared wavelengths (Van Buren 1993). Bow shocks around runaway OB stars have typically values of α between 0.01 and 0.1. As a group they should have very similar stability properties.

In Fig 3, we show a contour map of the bow shock associated with 'the runaway star ζ Oph (O9V, HD 149757) , based on the IRAS HIRES 60 μm image, which covers $\sim$ 20 x 30 arc minutes in the sky. This object is at a distance of $\sim$ 150 pc, with a terminal wind velocity $v_w \sim 1350$ km s^{-1} (Morton 1976), and a star velocity of $v_* \approx 30$ km S^{-1} (Gull & Sofia 1979), i.e. $\alpha \approx 0.02$.

It is difficult to find values of $\alpha > 1$ in most traditional stellar-ISM environments, nevertheless there mist a beautiful example near the Galactic center: the galactic center IRS 7 source (Yusef-Zadeh & Melia 1992). IRS 7 is a red supergiant located within 2 pc of the Galactic center (Sellgren et al. 1987) which shows a bow shock with its apex facing IRS 16 (a likely cluster of OB stars situated even closer to the Galactic center). In Fig 4 we show a contour map of 2 cm radio continuum of the IRS 7 bow shock from Yusef-Zadeh & Melia (1992). Its width at $\theta \sim 90^o$ is $\sim$ O." 34 and the map covers all area $\sim 1."5 \times 1."5$ on tile sky.

The bow shock arises in this case from the interaction of the red supergiant wind, $v_w \sim 30$ km s'-', with the IRS 16 wind "v_*" = 500 - 700 km s^{-1} (Yusef- Zadeh & Melia 1992), i.e. $\alpha \approx$ 16- 23. The IRS 7 bow shock displays a more clumpy structure than ζ

Oph, in accordance with its higher α and hence higher expected perturbation amplitude (See figure 2).

It is a pleasure to thank Ethan Vishniac and Mordecai Mark Mac-Low for a careful reading of the manuscript and many helpful comments. We want to thank Farhad Yusef-Zadeh for kindly making available to us his 1 RS 7 image in a very short notice. The research described in this paper was carried out by the Jet, Propulsion Laboratory, California, Institute of Technology, under a contract with the National Aeronautics and Space Administration. R.D. thanks the Swiss National Foundation for its support and the visiting scientist program at JPL. AN-C is supported by the NASA Long Term Astrophysics Program. The 60 μm image of ζ Oph was made possible through the support of the taxpayers of the US, UK and the Netherlands for the IRAS mission.

REFERENCES

Bairamov, Z. T., Pilyugin, N. N, & Usov, V. V., 1990, Soviet Physics-Doklady, 15,791

Baranov, V.B., Krasnobaev, K.V, & Kulikovskii, A.G., 1991, Sov. Astron., 34, 502

Brillouin, I,., 1926, Comptes. Rendus, 183, 24

Cruz-González, C., Recillas-Cruz, E., Costero, R., Peimbert, M., & Torres-Peimbert, S. 1974, RMxAA, 1, 211

Dgani, R.., 1993, A&A, 271, 527

Dgani, R., & Soker, N., 1994, A&A, 282, 54

Dgani, *R.*, Walder, R.,& Nussbaumer, H., *1993,* A&A, 267, 155

Giuliani, J.I,., 1982, ApJ 256, 624

Gull, T. R., & Sofia, S., 1979, ApJ, 230, 782

Kramer, H. A., 1926, Zeits. f. Physik, 38, 518

Mac-Low, M. M., Van Buren, D., Wood, 11.0. S., & Churchwell, E., ApJ, 369395

Mac-Low, M, M., & Norman, M. L., 1993, ApJ, 396,606

Morton D. 1976, ApJ, 203, 386

Ryu, D., Vishniac, E. T., 1988, ApJ, 331, 350

Soker, N., 1990, ApJ, 358, 545

Soker, N., 1991, ApJ, 376, 750

Sellgren, K., Hall, D. N. B., Kleinmann, S. G., & Scoville, N.Z. 1987, ApJ, 317, 881

Stevens, I. R., Blondin, J.M., Pollock, A. M. T., 1992, ApJ, 386, 265

Van Buren, J)., 1986, ApJ, 306, 358

Van Buren, D. & McCray, R. 1988, ApJ, 329, L93

Van Buren, D. 1993 in "Massive: Stars: Their Lives in the Interstellar Medium", ccl. J.P. Casinelli & E.B. Churchwell, ASPCS 35, 315

Van Buren, D., & Mac-Low, M. M., 1992, ApJ, 394, 534

Van Buren, D., Mac-Low, M. M., Wood, D.O. S., Churchwell, E. 1990, ApJ,R 353,570

Van Buren, D., Noriega-Crespo, A., & Dgani, R. 1995, AJ (in press)

Vishniac, E.T., 1994, ApJ, 428, 186

Wentzel, G., 1926, Zeits. f. Physik, 38, 518

Yusef-Zadeh, F., & Melia, F. 1992, ApJ, 385, L 41

FIGURE CAPTIONS

Figure 1. The coordinate system is shown.

Figure 2. Diagram of the relationship between the instability growth rate, $C(l)$, versus the star-wind velocity ratio α. The position for three different bow shocks with distinct α *values* (ζ Oph and IRS *7)* are marked.

Figure 3. A contour plot based on a high resolution 60μm 1 RAS image of ζ Oph (HD 149757). The motion of the star is along a $\sim$ 18° position angle, with a velocity of $\sim$25 km s^{-1}. The field is $\sim$ 30' x 20', north is up, east is left, tile contour levels are spaced a $2^1/2$ factor, and the cross marks the position of the star.

Figure 4. A contour map based continuum obser vations at a 2 cm wavelength of the IRS 7 bow shock in the Galactic. center (from Yusef-Zadeh & Melia 1992). The field is $\sim$1.″5 x 1.″5, and the contours are linearly space (see text for details).

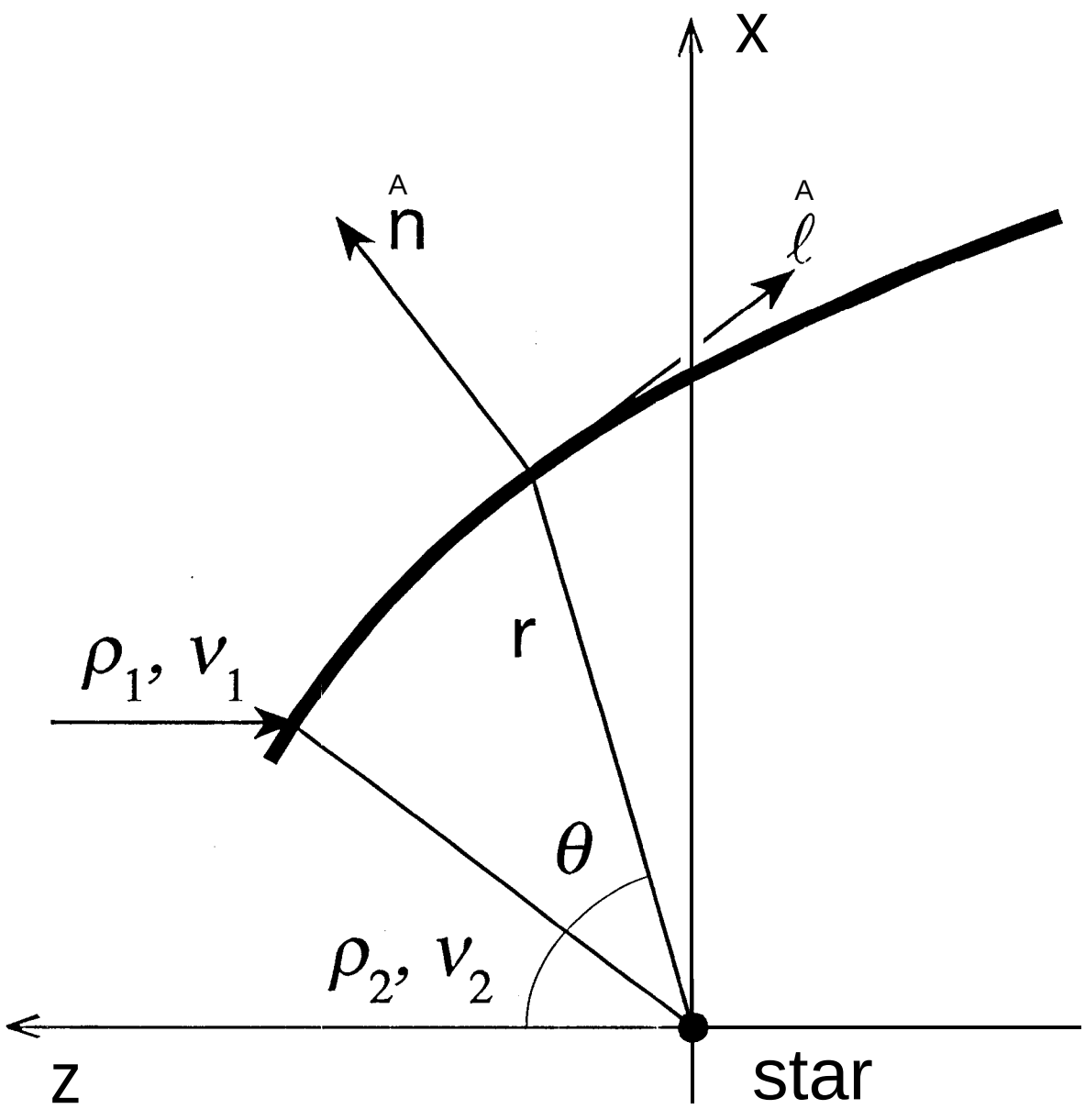

Fig. 1.

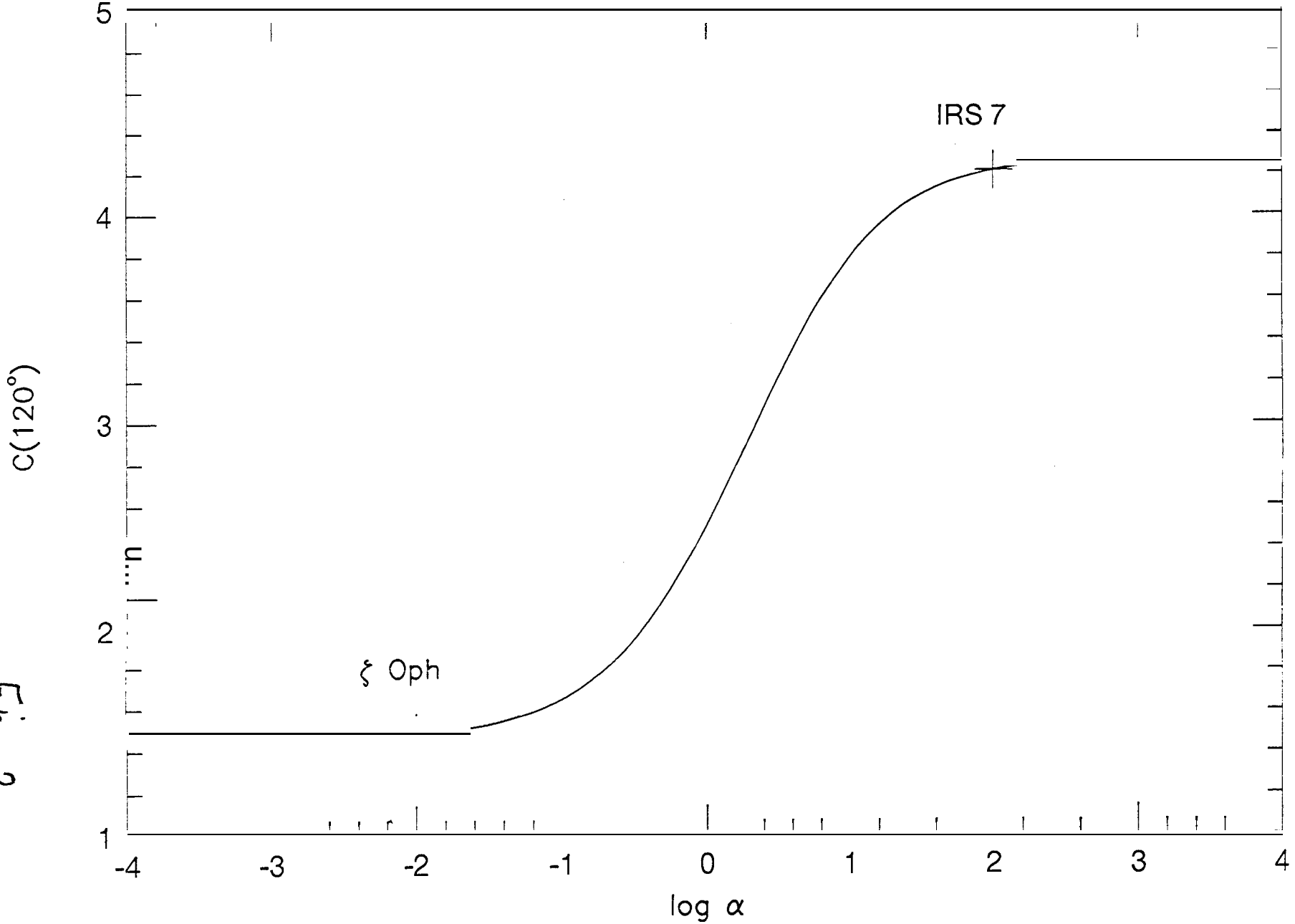
5
4
3
2
1
C(120°)
IRS 7
ζ Oph
-4
-3
-2
-1
0
1
2
3
4
log α

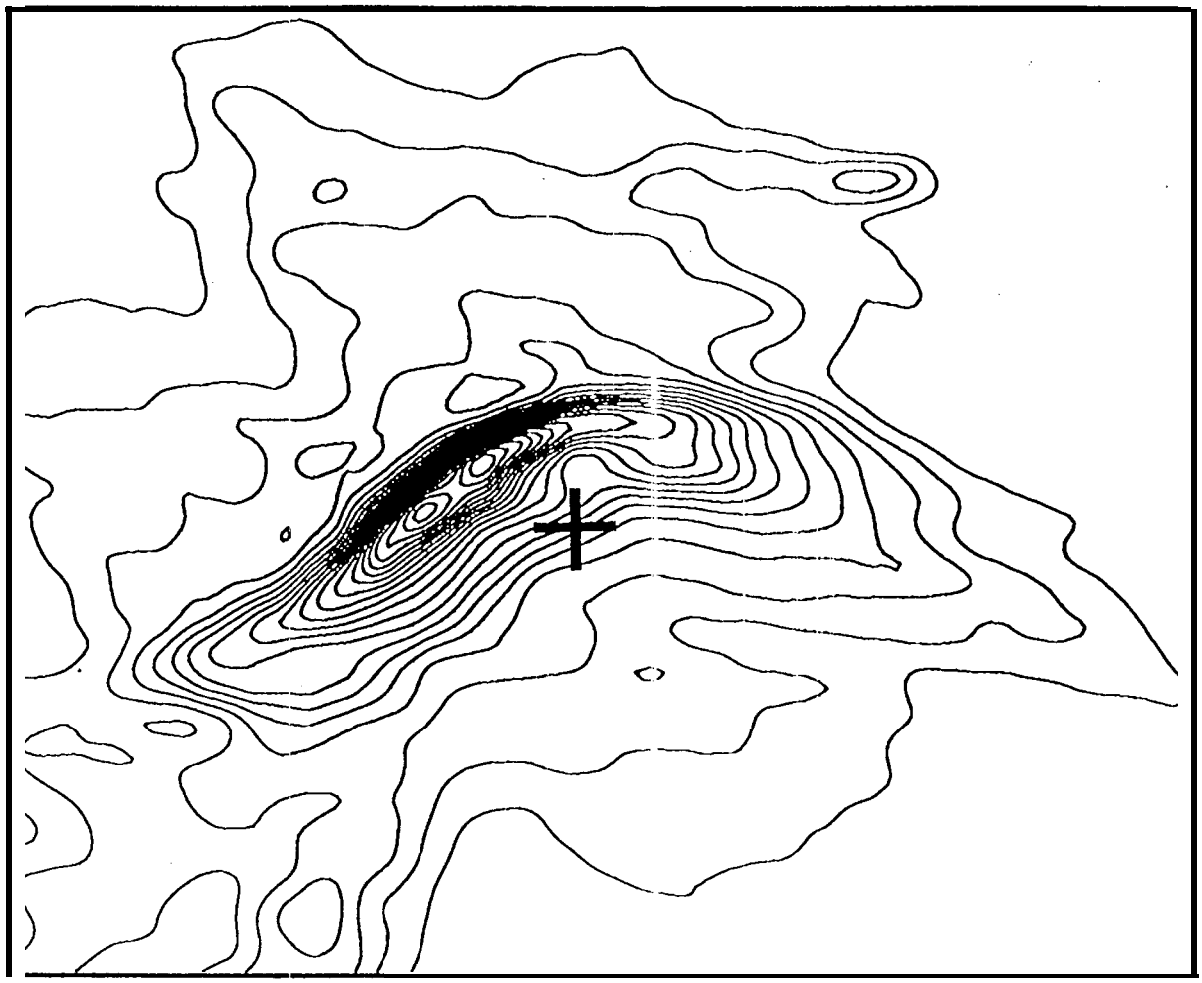

Fig. 3.

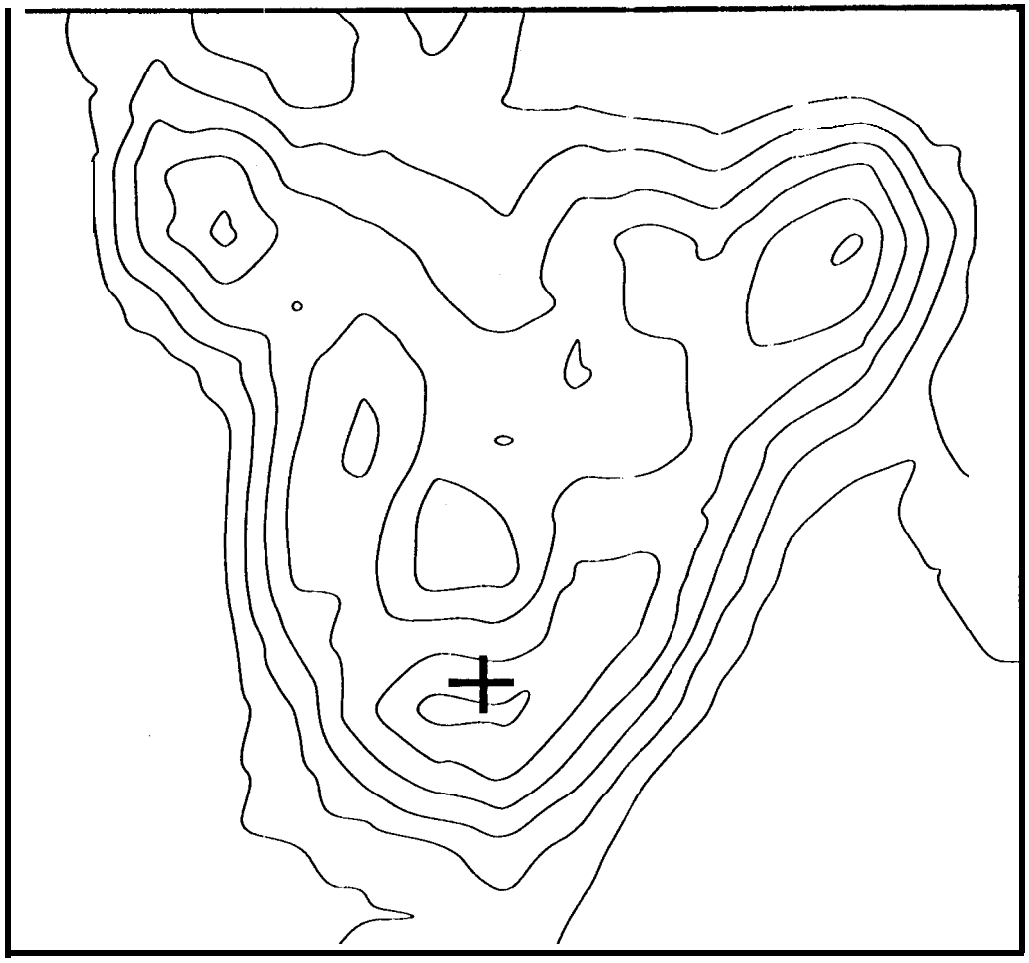

Fig. 4.